Available online at www.sciencedirect.com
SCIENCE DIRECT®
Sensors and Actuators B 107 (2005) 121–125
SENSORS AND ACTUATORS B CHEMICAL
www.elsevier.com/locate/snb

Two photon fluorescence sensors based on resonant grating waveguide structures

T. Katchalski[a], S. Soria[b,*], E. Teitelbaum[a], A.A. Friesem[a], G. Marowsky[c]

[a] *Department of Physics of Complex Systems, Weizmann Institute of Science, 76100 Rehovot, Israel*
[b] *ICFO-Institut de Ciències Fotòniques, E-08034 Barcelona, Spain*
[c] *Laser Laboratorium Goettingen e.V., Hans Adolf Krebs Weg 1, 37077 Goettingen, Germany*

Received 7 April 2004; received in revised form 21 June 2004; accepted 1 July 2004
Available online 14 November 2004

Abstract

We use novel high-finesse polymeric resonant grating waveguide structures (GWS) for strong enhancement of two photon fluorescence (TPF). At a specific wavelength and angular orientation of the incident beam, the grating waveguide structure resonates. This resonance results in a field enhancement at the surface that can be exploited for TPF spectroscopy, without the need for highly focused laser excitation light. We compare the TPF obtained from a thin layer of tetramethylrhodamine (TMR) deposited on top of a GWS at resonance and off-resonance. Our procedure and results indicate that the detection of TPF can indeed be improved with the resonant GWS by at least fifteen times. These results have been also demonstrated using a GWS and a 2 μm thick layer of TMR aqueous solution.

Keywords: Two photon fluorescence; Ultrafast lasers; Resonant phenomena

1. Introduction

Two photon fluorescence (TPF) measurements with near infra-red radiation (NIR) have a number of advantages over measurements with one photon excitation. Specifically, the large energy gap between the excitation and emission radiation reduces the background noise, the static photobleaching of the dyes that are used is reduced because there is a quadratic dependence of the absorption on intensity [1,2], and the use of near infra-red radiation minimizes the photodamage of cells and tissue thereby lowering autofluorescence. On the other hand, conventional TPF requires highly intense and focused laser light of instantaneous photon flux densities of at least 10^{31} photons/cm^2 s which in turn lowers the photodamage threshold [3]. In order to overcome such a difficulty, i.e. to achieve the needed energies and yet avoid tight focusing, we resort to low-loss, high-finesse resonant grating waveguide structures (GWS) [4,5].

The basic configuration of the GWS consists of a substrate, a waveguide layer and a grating layer on top. When the GWS is illuminated with an ultrashort light pulse, most of the light is directly transmitted through while some is diffracted by the grating, trapped in the waveguide layer, and subsequently partially rediffracted outwards. At a specific wavelength and angular orientation of the incident beam, the grating waveguide structure resonates, where the rediffracted beam destructively interferes with the transmitted beam and most of the incident light is reflected. Specifically, a very sharp decrease of the transmitted light is observed in the spectrum of the illuminating pulse.

For our purposes the most important feature of the GWS is the large optical field enhancement that can be achieved at the grating surface. Thus, the GWS can be exploited for two-photon fluorescence excitation of a layer deposited on top of the grating layer. The GWS have a number of additional attractive features for TPF applications. In particu-

* Corresponding author. Tel.: +34 93 4137942; fax: +34 93 4137943.
E-mail addresses: fetsvi@wisemail.weizmann.ac.il (T. Katchalski), silvia.soria@icfo.es (S. Soria).

0925-4005/$ – see front matter © 2004 Elsevier B.V. All rights reserved.
doi:10.1016/j.snb.2004.07.040

lar, they are compact and robust so as to simplify experimental set-ups, are relatively easy to fabricate, and can be readily incorporated into widespread biological and chemical applications. Our GWS were optimized for normal incidence of the excitation light, so are compatible with commercial instrumentation such as fluorescence scanners and microscopes.

In this paper, we first describe the resonant behaviour of the GWS with and without a tetramethylrhodamine (TMR) layer on top of its grating layer surface. Two types of layers have been investigated, a deposited TMR thin layer and a 2 μm thick layer of TMR aqueous solution. Then, we demonstrate TPF enhancement by measuring the TPF intensity at resonance and off-resonance. Finally, we measure the TPF signal as a function of central excitation wavelength and polarization.

2. Experimental set-up and procedure

The experimental set-up for evaluating the GWS and the two types of GWS arrangements are shown schematically in Fig. 1. The experimental set-up, shown in Fig. 1(a), includes a mode-locked Ti:Sapphire laser (Mira 900 F, Coherent) operated at a frequency of 76 MHz. The pulse width was 150 fs and the spectral bandwidth was about 8 nm. The excitation light wavelength could be tuned from 690 to 980 nm, but was generally centered at the resonant wavelength of the GWS. The GWS was mounted on a positioning stage (Physik Instrumente) which allowed for transverse translation and rotation in order to ensure accurate normal incidence. The TPF was collected by a spherical lens (f = 50 mm, NA = 0.8), focused onto the entrance slit of a spectrometer (Triax180, Jobin Ivon), and detected using a back-thinned CCD linear array (HC236-1007, Hamamatsu). The excitation light of the Ti:Sapphire was blocked by placing a NIR filter (BG39, Schott) in front of the entrance slit of the spectrometer.

Several GWS were fabricated. We used optical quality (λ/4) BK7 glass substrates onto which the waveguide and the photoresist layers were spin-coated. The waveguide layer consisted of a polyimide material of approximately 430 nm thickness (refractive index n = 1.7). The grating layer consisted of Shipley S1805 in which a surface relief grating was holographically recorded. Typically, the grating layer period was about 523 nm and the grating layer thickness was 450 nm. In principle, decreasing the grating thickness will narrow the resonance bandwidth, whereas changing the grating period will shift the resonance wavelength. The grating structure was optimized so as to minimize surface roughness, with different heat treatments, exposure, and development procedures. The waveguide layer also served as a stopping layer for the wet etching development of the grating layer and thus assisted in achieving a very uniform grating. Such uniformity in the grating layer essentially eliminates fluorescence crosstalk. Two types of TMR layers were then formed on top the GWS, as shown in Fig. 1(b). The first type of TMR layer was a 2 μm thick layer of a TMR aqueous solution obtained using a microfluidic cell enclosed on top of the GWS. This cavity was filled by capillary action with a 20 μM TMR solution. The second type of layer was obtained by depositing a drop of 15 μM TMR solution in milli-Q water (pH 7.5) on top of the GWS. After evaporation of the solvent, the TMR molecules remained immobilized on the GWS surface forming a uniform thin layer. The deposited TMR thin layer had an approximate thickness of 65 nm as measured with an alpha-step instrument. Fig. 2 shows a scanning electron microscope (SEM) image of the GWS with the

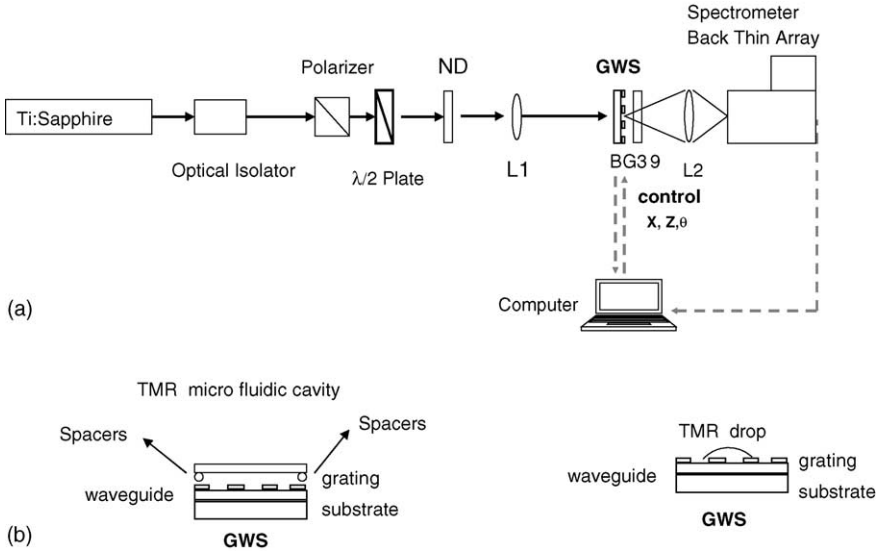

Fig. 1. Experimental arrangement for two photon fluorescence (TPF) evaluation of GWS and TMR layers. (a) Experimental TPF measurement set-up including, neutral density filters (ND), focusing lens (L1) and collecting lens (L2); (b) TMR deposited thin layer (right) and 2 μm thick TMR aqueous solution layer in a microfluidic cell configuration (left).

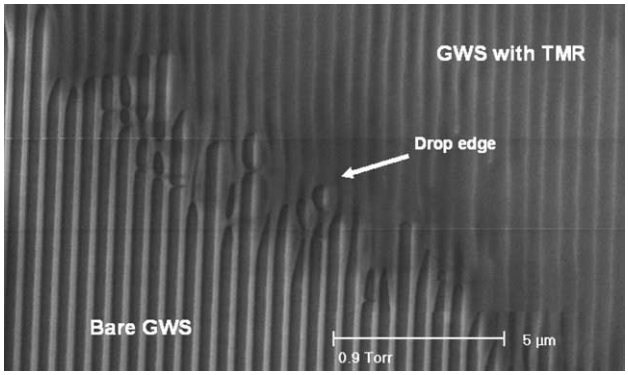

Fig. 2. SEM image of the grating layer and a TMR deposited thin layer on top. The edge of the thin layer divides the figure in two. The upper part of image is darker due to the additional thin layer.

deposited TMR thin layer. The edge of the drop divides the image in two where the upper part is darker due to the additional deposited TMR thin layer. Both types of TMR layers should lead to a shift of approximately 10 nm in the resonance wavelength due to the change of the optical parameters of the GWS.

3. Experimental results and discussion

Representative experimental results of the GWS spectral response and enhanced TPF are presented in Figs. 3 and 4. Fig. 3 shows the spectral response with and without a TMR layer. Fig. 3(a) shows the transmitted spectral response of the "bare" GWS, i.e. without TMR, the GWS with the adsorbed TMR thin layer and of the incident pulse, shown for reference. The transmitted spectral response of the GWS was obtained using normal incidence illumination. At the resonant wavelength, λ_{res} = 844 nm, for transverse electric (TE) polarization excitation, in which the electric field of the incident light is parallel to the grating grooves, the spectrum of the transmitted light shows a sharp decrease with a narrow resonance bandwidth of 2 nm at full-width half maximum (FWHM). For the transverse magnetic (TM) polarization excitation, shifts (not shown) by approximately 10 nm to a shorter wavelength as compared to TE polarization excitation. Thus it is possible to move from "at resonance" to "off-resonance" condition at a given wavelength just by changing from one polarization to the other. Indeed, for TM polarization at the same wavelength, i.e. off-resonance, the spectrum of the transmitted light corresponded to the full spectrum of the ultrashort pulse. Fig. 3(b) shows the transmitted spectral response of the GWS in contact with a relatively thick TMR aqueous solution layer in the microfluidic cavity configuration. In this case the resonant wavelength is centered at λ_{res} = 836 nm for TE polarization excitation and the resonance bandwidth at FWHM is 1 nm. The additional narrowing of the resonance bandwidth is due to the higher layer thickness above the GWS.

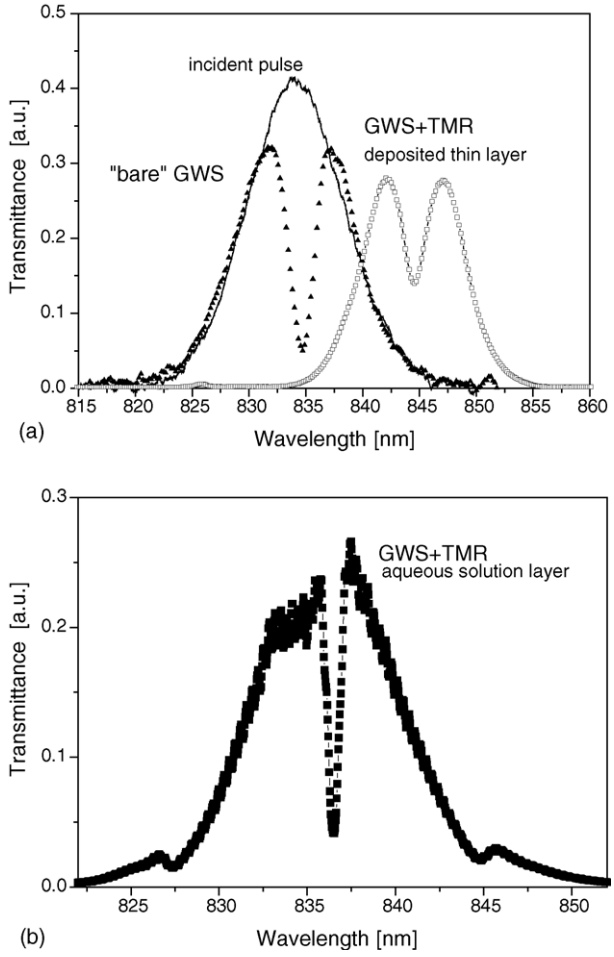

Fig. 3. Experimental measurements of the spectral response of GWS with and without TMR layers. (a) TE polarization excitation with resonance bandwidth at FWHM = 2 nm; "bare" GWS (triangles), GWS with deposited TMR thin layer (squares) and reference (solid line). For the "bare" GWS the transmission intensity drops by 90%; (b) GWS with 2 μm thick layer of TMR aqueous solution in a microfluidic cavity configuration. For TE polarization excitation, resonance wavelength, λ_{res} = 836 nm and resonance bandwidth at FWHM = 1 nm.

As evident from these experimental results, the transmitted intensities do not decrease to zero, indicating that our GWS has some loss. Since the absorption of polyimide and photoresist material for NIR wavelength is very small, we believe that the major source for loss are structural imperfections. For both types of TMR layers the resonance peak of the GWS with TMR layer is shifted to higher wavelengths compared to the bare GWS, as can be expected from numerical rigorous coupled wave analysis (RCWA) calculations.

Fig. 4 shows the TPF as a function of wavelength for different central excitation wavelengths, obtained with a GWS on which a TMR thin layer was deposited. In order to ensure that the fluorescence is indeed due to the GWS enhancement, we first tuned the incident laser wavelength from 830 to 856 nm at fixed polarization, and then varied the polarization at fixed wavelengths. The incident laser beam (240 mW) was

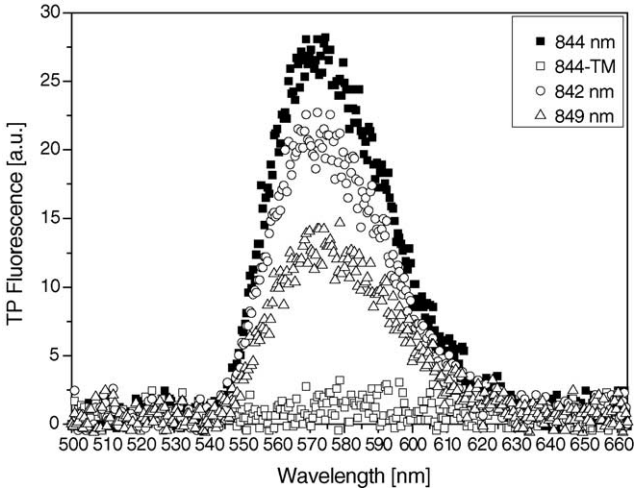

Fig. 4. Two Photon Fluorescence (TPF) emission spectra of GWS with TMR deposited thin layer at different excitation wavelengths. Excitation wavelength at resonance $\lambda = 844$ nm, TE-mode (filled squares); off-resonance, $\lambda = 844$ nm, TM-mode (empty squares); maximum two photon absorption $\lambda = 849$ nm, TE-mode (triangles); excitation at twice FWHM from resonance, $\lambda = 842$ nm, TE-mode (circles).

slightly focused to a 100 μm beam waist. As evident, near and at resonance the TPF from the GWS could be readily observed. On the other hand, far away from resonance no TPF signal could be observed. Near resonance, the TPF intensity increases strongly, reaching its maximum at the resonance wavelength of 844 nm, indicating a strong field enhancement. Also shown are TPF signals obtained at 849 nm, the maximum TPF absorption wavelength, and at 842 nm which is two FWHM away from the resonance excitation wavelength. The TPF signal at the excitation wavelength of 844 nm (suitable for resonance with TE polarization) was detected as background noise signal for TM polarization. Similarly, no TPF was detected when using a reference glass with a deposited TMR thin layer under identical experimental conditions, indicating clearly the enhancement of the TPF detection with GWS.

To quantify the TPF enhancement, we integrated the TPF signal as a function of wavelength for each excitation wavelength. The results are presented in Fig. 5. Since the TPF signal is proportional to the convolution of the GWS transmission spectrum and the pulse intensity envelope, considerable TPF signal is also present at wavelengths close to the resonance wavelength. Since the resonance bandwidth is considerably narrower than the pulse envelope the TPF signal is expected to resemble a slightly broadened pulse envelope. As evident in Fig. 5(a), the integral TPF signal is centered at the resonance wavelength of the GWS and has an envelope resembling the excitation pulse envelope. The ratio of resonance/off-resonance TPF integral signal is as high as 15. The integral TPF signal obtained for the GWS with the 2 μm thick TMR aqueous solution layer are shown in Fig. 5(b). In this case, the maximum TPF intensity is observed at the resonance wavelength of $\lambda_{res} = 836$ nm. The results are similar

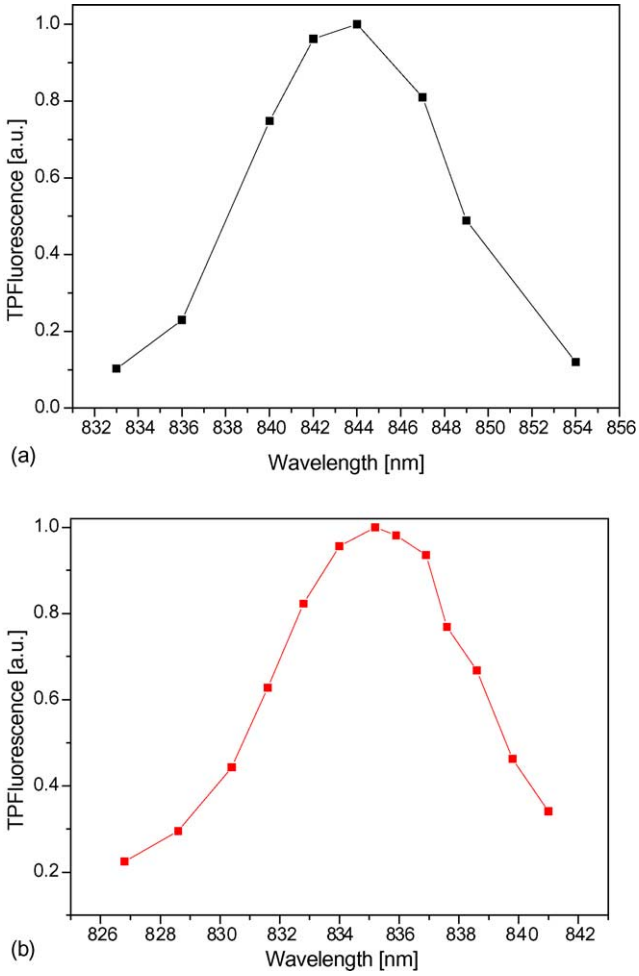

Fig. 5. Integral TPF signal as a function of central excitation wavelength of a GWS. (a) with TMR deposited thin layer; (b) with 2 μm thick TMR aqueous solution layer.

to those obtained with the deposited TMR thin layer. No TPF was detected in the spectral region between 350 and 500 nm or in regions without the immobilized TMR. Thus, one can exclude other nonlinear effects like surface second harmonic generation [6].

4. Concluding remarks

Our procedure and results indicate that the detection of TPF can indeed be more sensitive with the resonant GWS. We expect that the overall detection sensitivities can increase even further as the fabrication of the GWS is improved, so they can be incorporated into fluorescence based sensors and open up new options for medical diagnostics.

Acknowledgements

S.S. acknowledges funding from the Generalitat de Catalunya and from the Ministerio de Ciencia y Tecnolo-

gia through the Ramon y Cajal program. The work was supported in part by VDI (Verein Deutscher Ingenieure) grant GILCULT 13N7963. We would like to thank Prof. H.G. Weber and his group of the Fraunhofer Heinrich-Hertz-Institut, Berlin, Germany and Prof. J. Zyss and his group of Laboratoire de Photonique Quantique et Moleculaire, ENSC, Cachan, France, for the long on-going fruitful collaboration on GWS.

References

[1] W. Denk, J.H. Strickler, W.W. Webb, Two-photon laser scanning microscopy, Science 248 (1990) 73–76.

[2] P. Schwille, U. Haupts, S. Maiti, W.W. Webb, Molecular dynamics in living cells observed by fluorescence correlation spectroscopy with one- and two-photon excitation, Biophys. J. 77 (1999) 2251–2265.

[3] P.S. Dittrich, P. Schwille, Photobleaching and stabilization of fluorophores used for single-molecule analysis with one- and two-photon excitation, Appl. Phys. B 73 (2001) 829–837.

[4] A. Donval, E. Toussaere, J. Zyss, G. Levy-Yurista, E. Jonsson, A.A. Friesem, Novel polymer-based resonant grating-waveguide structures, Synth. Met. 124 (2001) 19–22.

[5] A. Sharon, D. Rosenblatt, A.A. Friesem, Resonant grating-waveguide structures for visible and near-infrared radiation, J. Opt. Soc. Am. A 14 (1997) 2985–2993.

[6] G.L. Duveneck, M.A. Bopp, M. Ehrat, M. Haiml, U. Keller, M.A. Bader, G. Marowsky, S. Soria, Evanescent-field-induced two-photon fluorescence: excitation of macroscopic areas of planar waveguides, Appl. Phys. B 73 (2001) 869–871.